

A tale of two beams: an elementary overview of Gaussian beams and Bessel beams

ROBERT L. NOWACK

Department of Earth and Atmospheric Sciences, Purdue University, West Lafayette, IN 47907, USA
(nowack@purdue.edu)

Received: September 5, 2011; Revised: January 5, 2012; Accepted: January 12, 2012

ABSTRACT

An overview of two types of beam solutions is presented, Gaussian beams and Bessel beams. Gaussian beams are examples of non-localized or diffracting beam solutions, and Bessel beams are example of localized, non-diffracting beam solutions. Gaussian beams stay bounded over a certain propagation range after which they diverge. Bessel beams are among a class of solutions to the wave equation that are ideally diffraction-free and do not diverge when they propagate. They can be described by plane waves with normal vectors along a cone with a fixed angle from the beam propagation direction. X-waves are an example of pulsed beams that propagate in an undistorted fashion. For realizable localized beam solutions, Bessel beams must ultimately be windowed by an aperture, and for a Gaussian tapered window function this results in Bessel-Gauss beams. Bessel-Gauss beams can also be realized by a combination of Gaussian beams propagating along a cone with a fixed opening angle. Depending on the beam parameters, Bessel-Gauss beams can be used to describe a range of beams solutions with Gaussian beams and Bessel beams as end-members. Both Gaussian beams, as well as limited diffraction beams, can be used as building blocks for the modeling and synthesis of other types of wave fields. In seismology and geophysics, limited diffraction beams have the potential of providing improved controllability of the beam solutions and a large depth of focus in the subsurface for seismic imaging.

Keywords: Gaussian beams, Bessel beams, Bessel-Gauss beams, wave propagation

1. INTRODUCTION

Gaussian beams are solutions to the wave equation that stay bounded for some propagation range after which they diverge (Siegman, 1986). In the 1980's, Durnin (1987) and Durnin et al. (1987) showed that certain types of beams could propagate without changing shape for large distances and were called Bessel beams. These solutions were found earlier by Stratton (1941), Courant and Hilbert (1966) and Bateman (1915) among others, and recent overviews are given by McGloin and Dholakia (2005), Recami et al. (2008), Recami and Zamboni-Rached (2009, 2011) and Turunen and Friberg (2010). These solutions however are endowed with infinite energy, similar to plane waves, and

did not attract much interest until more recently when experimental results were obtained. In this overview, I will first describe Gaussian beams as examples of beams solutions that diffract as they propagate. These are then contrasted with Bessel beams as examples of wave solutions with limited diffraction properties. For pulsed beams, these result in X-wave solutions. Gaussian beams have been extensively utilized for geophysical modeling and imaging as illustrated by the recent conference on localized waves in Sanya, China (*ISGILW-Sanya2011, 2011*). Although limited diffraction beams have been well studied in optics and acoustics, they have so far not seen any significant applications in seismology and geophysics. For example, at the recent Sanya conference only several presentations discussed limited-diffraction localized beams (e.g. *Recami, 2011; Zheng et al., 2011*). In addition to presenting an elementary overview of Gaussian beams, Bessel Beams, and Bessel-Gauss beams, I will also briefly discuss seismic imaging using beam solutions and potential applications of limited diffraction beams for this.

2. GAUSSIAN BEAMS AS NON-LOCALIZED BEAM SOLUTIONS

Gaussian beams are example of non-localized beam solutions that diffract as they propagate, and can be derived in several ways (*Siegman, 1986*). These include the complex source point approach in which an analytic continuation of a point source from a real source location (x_1^0, x_2^0, x_3^0) to a complex location $(x_1^0, x_2^0, x_3^0 + ib)$ is performed. The solution for a point source e^{ikR}/R , where k is the wavenumber, is then modified to a Gaussian beam solution with x_3^0 replaced by $x_3^0 + ib$ (e.g., *Deschamps, 1971; Keller and Streifer, 1971; Felsen, 1976; Wu, 1985*), and this can be used to extrapolate analytical formulations of wave solutions for point sources to Gaussian beams. Other approaches to derive Gaussian beams include the differential equation approach based on the paraxial wave equation, the Huygens-Fresnel integral with an initial Gaussian amplitude profile, a plane wave expansion approach, and solutions to the Helmholtz equation in oblate spheroidal coordinate systems.

Gaussian beams in homogeneous media can be written as (*Siegman, 1986*)

$$u(r, x_3) = \left(\frac{2}{\pi}\right)^{\frac{1}{2}} \frac{W_0}{W(x_3)} e^{ikx_3 + \frac{ikr^2}{2R(x_3)} - i\psi(x_3)} e^{\frac{-r^2}{W^2(x_3)}}, \quad (1)$$

where x_3 is the direction of propagation, $k = \omega/v$ is the wavenumber with ω the radial frequency and v the wave speed, and $r = (x_1^2 + x_2^2)^{1/2}$ is the transverse distance to the direction of propagation. $W(x_3) = W_0 \left(1 + (x_3/X_3^R)^2\right)^{1/2}$ is the beam width where the amplitude decays in the transverse direction to $1/e$, and W_0 is the beam width at the beam-waist specified here at $x_3 = 0$. Also, $X_3^R = \pi W_0^2/\lambda$ is the Rayleigh range where

the amplitude decays to $1/e$ at a transverse distance of $r = \sqrt{2}W_0$, and λ is the wavelength. The radius of curvature of the beam is $R(x_3) = x_3 \left(1 + \left(X_3^R / x_3 \right)^2 \right)$. The beam is narrowest for the beam-waist at $x_3 = 0$, and also the phase front is planar with $R(x_3) = \infty$. As $|x_3| \rightarrow \infty$, the radius of curvature also goes to infinity. The radius of curvature is smallest (maximum curvature) at the Rayleigh range X_3^R . $\psi(x_3)$ is called the Gouy phase, and for a Gaussian beam in a homogeneous medium is equal to $\psi(x_3) = \tan^{-1} \left(x_3 / X_3^R \right)$.

Fig. 1 illustrates the characteristics of a Gaussian beam in a homogeneous medium with a velocity of $v = 5$ km/s appropriate for the Earth's upper crust. The frequency f is specified as 1 Hz, and the initial beam width W_0 is 7.5 km. The range over which the beam stays bounded in transverse distance is between $-X_3^R < x_3 < X_3^R$, and the far field angular spread of the beam is $\theta_G = \lambda / \pi W_0$. Fig. 2 displays the beam width with propagation distance of two Gaussian beams for different initial beam widths W_0 of 3.25 and 7.5 km, again with $v = 5$ km/s and $f = 1$ Hz. This shows that as the initial beam width W_0 gets smaller, the far field angular spread of the beam θ_G gets larger and the bounded Rayleigh range gets smaller.

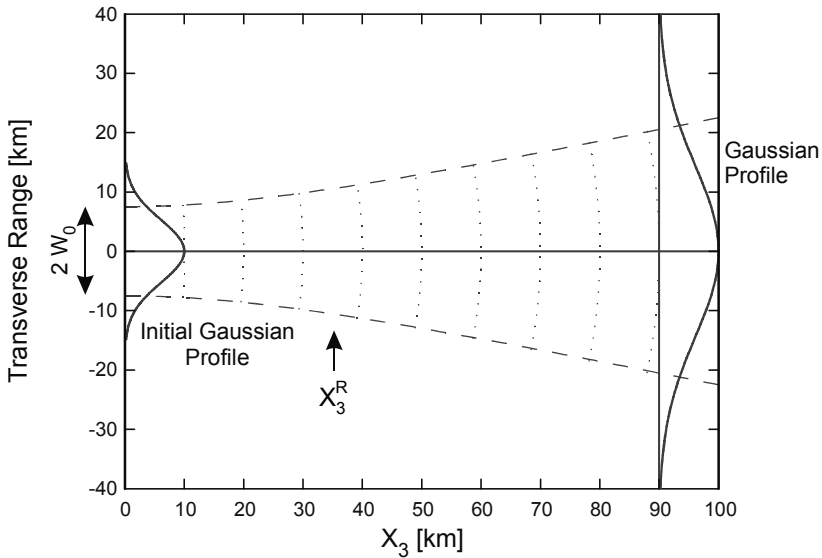


Fig. 1. Characteristics of Gaussian beam propagation in a homogeneous medium with $v = 5$ km/s, $f = 1$ Hz, and an initial beam width W_0 of 7.5 km.

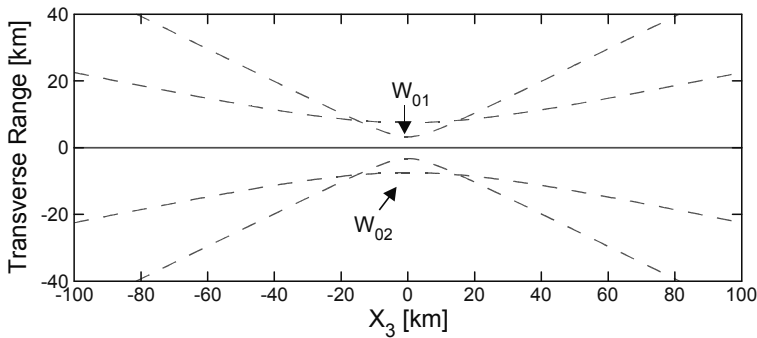


Fig. 2. Diffraction spreading of two Gaussian beams in a homogeneous medium with $v = 5$ km/s, $f = 1$ Hz, and two different initial beam widths $W_{01} = 3.25$ and $W_{02} = 7.5$ km.

The oblate spheroidal coordinate system well represents the shape of a Gaussian beam and can be used to derive Gaussian beam solutions to the Helmholtz equation. These coordinates were originally used in antenna theory (e.g. *Stratton, 1956; Flammer, 1957*), and a recent overview of wave solutions in oblate spheroidal coordinates is given by *McDonald (2002)*.

All waves that go through a focus experience a phase advance called the Gouy phase $\psi(x_3)$. *Feng and Winful (2001)* inferred that for a Gaussian beam, this results from the lateral beam spread as the wave emanates from the beam waist. For a Gaussian beam, this phase shift is progressive from 0 to $\pi/2$ from the beam waist for $0 < x_3 < \infty$ ($\pi/4$ for each lateral dimension). In Huygens-Fresnel integrals of a wavefront in terms of secondary wavelets, a $\pi/2$ phase shift is also required between the incident wavefront and the diverging secondary wavelets. For $-\infty < x_3 < +\infty$, the Gouy phase results in a phase shift of π for a 3D wave going through a focus ($\pi/2$ for a 2D beam), and for Gaussian beams this is again progressive with distance (*Nowack and Kainkaryam, 2011*).

Paraxial Gaussian beams in inhomogeneous media can be described by dynamic ray tracing with complex initial conditions along a real central ray, and this provides a major computational advantage for the calculation of high-frequency Gaussian beams in smoothly varying media with interfaces. Overviews of paraxial Gaussian beams using dynamic ray tracing are given by *Červený (2001)*, *Popov (2002)* and *Kravtsov and Berczynski (2007)*. *Popov (1982)* and *Červený et al. (1982)* developed summation methods in which Gaussian beams were used for the synthesis of other types of wavefields (for reviews see, *Babich and Popov, 1989; Popov, 2002; Nowack, 2003* and *Červený et al., 2007*). *Hill (1990, 2001)* developed a method using Gaussian beams for the migration imaging of seismic reflection data. This was extended to anisotropic media by *Alkhalifah (1995)*, to common-shot data by *Nowack et al. (2003)* and *Gray (2005)*, and for true-amplitude migration by *Gray and Bleistein (2009)*. For these approaches, the beams were launched into the subsurface at the source and receiver arrays along the surface, and the beam-waists were also specified at the surface. *Protasov and Cheverda (2006)*, *Popov*

et al. (2010) and *Protasov and Tcheverda* (2011) developed Gaussian beam migration approaches with the beams launched upwards from the individual subsurface scattering points to the surface, and the beam-waists were specified at the subsurface scattering points. These approaches provide more control of the beams at the scattering points, but are more computationally intensive than the previous approaches and the beams still diffract and broaden as they propagate through the medium.

An application of wave packets to migration imaging was given by *Douma and de Hoop* (2007) where the wavefield data was first decomposed into curvelets which were then sheared and translated in the imaging process. However, this approach did not include diffraction and curvature effects of the individual curvelets during propagation. A higher order development was presented by *de Hoop et al.* (2009) using wave packets which allowed for curvature effects during propagation more reminiscent of Gaussian beams. An alternative approach for the decomposition of wavefields into optimized Gaussian wave packets was developed by *Žáček* (2006).

Migration imaging was implemented by *Nowack* (2008) with Gaussian beams launched from the source and receiver arrays at the surface, but with the narrow and planar beam-waists focused to occur in the subsurface. This was extended by *Nowack* (2011) to allow for dynamic focusing at all sub-surface points giving the effect of diffraction-free beam propagation in the resulting image. However, this was only an apparent effect resulting from the use of multiple focusing points in the subsurface. The advantage of using dynamic focused of beams launched from the surface versus approaches that launch beams from the subsurface scattering points is computational speed, but this approach is still slower than approaches with beams launched from the surface either with beam-waists specified at the surface or by using single focusing depths.

In contrast to Gaussian beams, Bessel beams described next are examples of solutions to the wave equation that ideally do not diffract as they propagate. As a consequence they have the potential of providing better controllability of the beam solutions during propagation and a wide depth of focus for seismic imaging applications.

3. BESSEL BEAMS AS LOCALIZED BEAM SOLUTIONS

Bessel beams are among a class of localized beams solution which ideally do not spread with propagation distance. In the 1980's there was an interest in non-diffracting beam solutions which included focus wave modes (*Brittingham, 1983*), exact wave solutions with complex source locations (*Ziolkowski, 1985*), and also solutions called electromagnetic missiles (*Wu, 1985*). *Durnin (1987)* and *Durnin et al. (1987)* showed that Bessel beams can propagate without change of shape to a large range in free space. These types of beams were described earlier, for example by *Stratton (1941)*, *Courant and Hilbert (1966)* and *Bateman (1915)* among others, but because of their infinite energy (like plane waves), did not attract much interest at the time. To derive these solutions, consider the scalar wave equation,

$$\frac{1}{v^2} \frac{\partial^2 u}{\partial t^2} = \nabla^2 u . \quad (2)$$

A trial solution can be used of the form

$$u(x,t) = f(r)e^{i(k_3x_3 - \omega t)}, \tag{3}$$

where $r = (x_1^2 + x_2^2)^{1/2}$ is the transverse distance and the lateral shape $f(r)$ is preserved with propagation distance x_3 . Substituting this trial solution into the wave equation results in

$$r^2 \frac{d^2 f(r)}{dr^2} + r \frac{df(r)}{dr} + r^2 (k^2 - k_3^2) f(r) = 0, \tag{4}$$

where $k^2 = \omega^2/v^2$. Recall Bessel's equation (for example, *Weber and Arfken, 2004*)

$$x^2 \frac{dJ_\nu(x)}{dx^2} + x \frac{dJ_\nu(x)}{dx} + (x^2 - \nu^2) J_\nu(x) = 0, \tag{5}$$

where $J_\nu(x)$ is a cylindrical Bessel function of order ν . Fig. 3 shows cylindrical Bessel functions of several orders. For Eq.(4), one solution is $f(r) = J_0(k_r r)$ where $k_r^2 = k^2 - k_3^2$. Therefore, a solution to the wave equation in free space that doesn't change lateral shape with distance is

$$u(x,t) = J_0(k_r r) e^{i(k_3x_3 - \omega t)}, \tag{6}$$

where $k^2 = \omega^2/v^2 = k_1^2 + k_2^2 + k_3^2 = k_r^2 + k_3^2$. With $k_r = k \sin \theta$ and $k_3 = k \cos \theta$, then

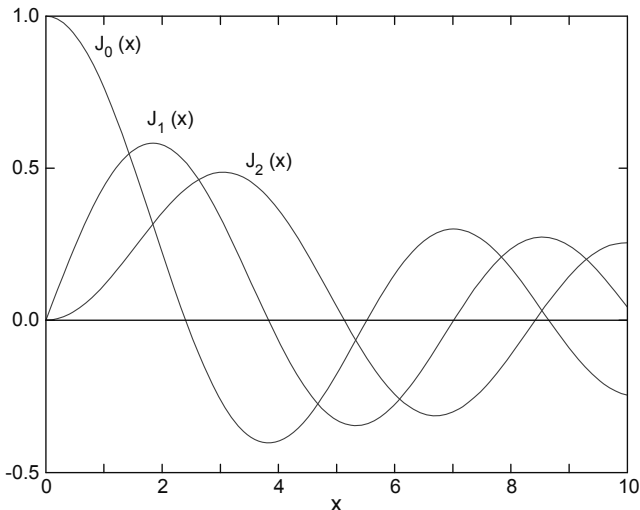


Fig. 3. Cylindrical Bessel functions of different orders. The horizontal axis is with respect to the argument of the Bessel functions.

$$u(x, t) = J_0(k \sin \theta r) e^{i(k \cos \theta x_3 - \omega t)}, \quad (7)$$

for a given angle θ . For $\theta = 0$, the solution reduces to a plane wave propagating in the x_3 direction. The first zero of the central lobe of the zeroth-order Bessel function is at $r = 2.4/(k \sin \theta)$. Thus, a more narrow central lobe will result by either increasing the radial frequency ω which increases k , or by increasing θ .

To show that this solution can be described in terms of plane waves, the Bessel function can be written as

$$J_0(r) = \frac{1}{2\pi} \int_0^{2\pi} d\alpha e^{ir \cos \alpha}. \quad (8)$$

Let $\alpha = \varphi - \varphi'$, then $\cos \alpha = \cos(\varphi - \varphi') = \cos \varphi \cos \varphi' + \sin \varphi \sin \varphi'$. Also, let $x_1 = r \cos \varphi'$ and $x_2 = r \sin \varphi'$, then

$$J_0(r) = \frac{1}{2\pi} \int_0^{2\pi} d\varphi e^{i(\cos \varphi x_1 + \sin \varphi x_2)}. \quad (9)$$

Now considering

$$u(x, t) = J_0(k \sin \theta r) e^{i(k \cos \theta x_3 - \omega t)}, \quad (10)$$

then

$$u(x, t) = \int_0^{2\pi} d\varphi e^{i(k \sin \theta \cos \varphi x_1 + k \sin \theta \sin \varphi x_2 + k \cos \theta x_3 - \omega t)}. \quad (11)$$

This then equals

$$u(x, t) = \int_0^{2\pi} d\varphi e^{i\vec{k} \cdot \vec{x} - \omega t}, \quad (12)$$

where the integrand is now in the form of plane waves with $\vec{k} = (\omega/v)(\sin \theta \cos \varphi, \sin \theta \sin \varphi, \cos \theta)^T$. Eq.(12) defines a cone of plane waves with normals with respect to the x_3 axis (Fig. 4). This cone of plane wave normals or a conical wave creates a Bessel beam which has a lateral cross-section which is invariant with propagation distance, and results in an ideal diffraction-free beam solution of the wave equation in free space.

The transverse cross-section is a Bessel function and for intensity this is shown in Fig. 5. Like a plane wave, ideal Bessel beams have infinite energy and propagate in a diffraction free manner. A Bessel beam can be formed in several ways. *Durnin et al. (1987)* used an annular aperture followed by a lens to construct Bessel beams. Bessel

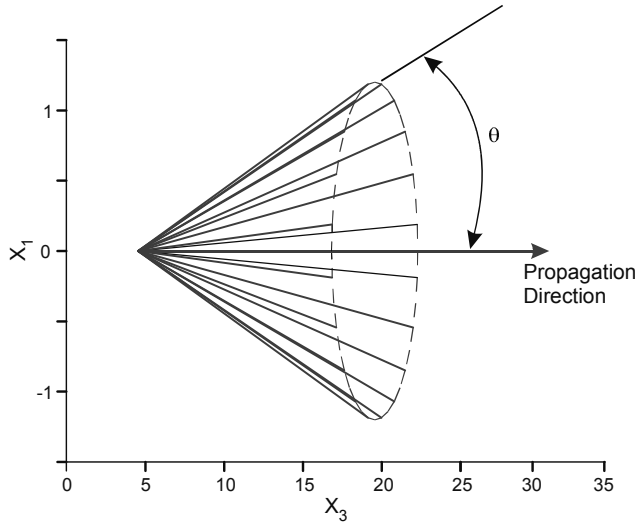


Fig. 4. Plane wave normal vectors along a cone making up a non-diffracting Bessel beam. All the plane waves of the Bessel beam have the same inclination angle θ_0 with respect to the propagation axis X_3 , where X_1 is the transverse coordinate and both are in arbitrary distance units.

beams can also be formed by a so-called axicon lens (McGloin and Dholakia, 2005) (see also Mcleod, 1954, 1960; Burckhardt et al., 1973; Sheppard, 1978 and Sheppard and Wilson, 1978). In each of these cases, the diffraction free range x_3^{max} is limited practically by the size of the lens R , where $x_3^{max} = R/\tan \theta$ and θ is the opening angle of the beam. Bouchal (2003) showed various kaleidoscope patterns for non-diffracting beams formed from discrete sets of plane waves at a fixed opening angle from the propagation direction.

Bessel beams are free-wave mode solutions in a cylindrical coordinate system, and therefore can be used to decompose other cylindrically symmetric wavefields. For example, a spherical wave can be decomposed into plane waves as

$$\frac{e^{i\omega R/v}}{R} = \frac{i}{2\pi} \int_{-\infty}^{\infty} dk_1 \int_{-\infty}^{\infty} dk_2 \frac{1}{k_3} e^{i(k_1 x_1 + k_2 x_2 + k_3 |x_3|)}, \quad (13)$$

where $k_3 = (\omega^2/v^2 - k_1^2 - k_2^2)^{1/2}$ with $\text{Im}(k_3) > 0$ and $\text{Re}(k_3) > 0$, which is called the Weyl integral (Aki and Richards, 1980; Chew, 1990). A spherical wave can also be written as

$$\frac{e^{i\omega R/v}}{R} = i \int_0^{\infty} dk_r \frac{k_r}{k_3} J_0(k_r r) e^{ik_3 |x_3|}, \quad (14)$$

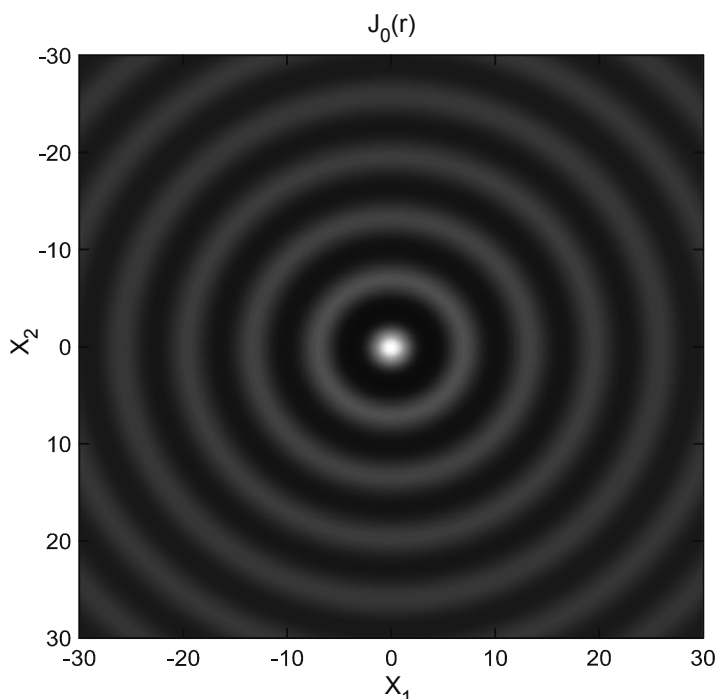


Fig. 5. The transverse intensity pattern of a zeroth-order Bessel beam. The axes are with respect to the argument of the Bessel function.

which is called the Sommerfeld integral (*Aki and Richards, 1980; Chew, 1990*) and is a decomposition of a spherical wave into cylindrical or conical waves. This can also be written in terms of Hankel functions of the first and second kind where $J_0(x) = \frac{1}{2} \left(H_0^{(1)}(x) + H_0^{(2)}(x) \right)$, as can Bessel beams (*Chavez-Cerda, 1999*). Eqs.(13) and (14) are both very commonly used in seismology and geophysics in reflectivity methods which decompose spherical waves into either plane waves or conical waves and then either transmit, reflect and reverberate these waves in a layered medium (*Aki and Richards, 1980*).

For pulsed Bessel beams, researchers have found so-called “X-waves” which travel in the shape of an “X” in the x_3 direction. In acoustics, these were first experimentally observed by *Lu and Greenleaf (1992a,b)* based on work performed at the Mayo Clinic (see also, *Lu and Greenleaf, 1994; Lu, 2008*). *Saari and Reivelt (1997)* experimentally observed Bessel X-wave propagation for light propagation. Localized X-shaped solutions to Maxwell’s equations for electromagnetism were described by *Recami (1998)*, and more general X-shaped waves were subsequently constructed with finite total energies and arbitrary frequencies (e.g. *Zamboni-Rached et al., 2002*). Similarities and differences

between Cherenkov-Vavilov radiation and X-shaped localized waves were discussed by Walker and Kuperman (2007) and Zamboni-Rached et al. (2010).

Recami et al. (2008) gave the frequency-wavenumber spectrum of an ideal harmonic Bessel beam as

$$S(k_r, \omega) = \frac{\delta\left(k_r - \frac{\omega}{v} \sin \theta\right)}{k_r} \delta(\omega - \omega_0), \quad (15)$$

where this describes a cone in wave-number space with $k_r^2 = k_1^2 + k_2^2$ at a single frequency ω_0 . For an X-shaped pulsed beam, this can be written as

$$S(k_r, \omega) = \frac{\delta\left(k_r - \frac{\omega}{v} \sin \theta\right)}{k_r} F(\omega), \quad (16)$$

where $F(\omega)$ describes the frequency spectrum of the pulsed signal.

“Superluminal” behavior for non-diffracting beam solutions (or faster than light speed or medium speed in acoustics) has been described by many authors (for example see Mugnai et al., 2000). Since a zeroth-order Bessel beam can be written as

$$u(x, t) = J_0(k \sin \theta r) e^{i(k \cos \theta x_3 - \omega t)}, \quad (17)$$

the apparent phase velocity of the Bessel beam v^{bb} in the x_3 direction can be obtained from

$$k_3 x_3 = k \cos \theta x_3 = \frac{\omega}{v} \cos \theta x_3 = \frac{\omega x_3}{v^{bb}}, \quad (18)$$

as $v^{bb} = v/\cos \theta$ where v is the medium velocity. Therefore, for $\theta > 0$, then $v^{bb} > v$.

For a single oblique plane wave making up a simple Bessel beam, phase velocities faster than the medium velocity are familiar to seismologists and geophysicists from seismic waves that are obliquely incident at a seismic array. Another example is that of ocean waves obliquely incident on a beach with the apparent phase speed along the beach greater than the wave speed. However, from Eq.(18) for Bessel beams,

$$v_g^{bb} = \frac{\partial \omega}{\partial k_3} = \frac{\partial}{\partial k_3} (v^{bb} k_3) = v^{bb} > v$$

implying superluminal group velocities as well. This has been addressed by a number of authors (see for example, McDonald, 2000; Sauter and Paschke, 2001; Lunardi, 2001). For example, Sauter and Paschke (2001) defined a different energy velocity as $v_e^{bb} = v \cos \theta$ for the package of oblique plane waves making up the Bessel beam, and for nonzero θ this is less than the medium velocity v . McDonald (2000) discussed this in terms of interference phenomena making up the Bessel beam and noted that

“superluminal behavior does not violate special relativity, but is rather an example of the ‘scissors paradox’ that the point in contact of a pair of scissors can move faster than the speed of light while the tips of the blades are moving together at sub-light speed.” As a result of these controversies, different definitions of signal velocities have been reassessed (e.g. Milonni, 2005), and there has been a renewed interest in classic work on wave speeds, such as that of Brillouin (1960).

As an example, Fig. 6 shows a central pulse formed from the crossing of two plane waves in 2D (from Sauter and Paschke, 2001). The overall shape of the central pulse moves in the vertical x_3 direction without change of shape. In an actual X-wave, this would result in a pulsed solution from the superposition of plane waves over the complete cone with a fixed angle from the propagation direction. The central pulse of the “X” moves in the vertical x_3 direction at a speed of $v/\cos\theta > v$. However, this speed is only apparent since different parts of the planar wavefronts making up the center of the “X” pulse come from different points along the intersecting plane waves at different times and don’t constitute the actual propagation of the same signal along the center of the “X” pulse. However, this effect can also result in interesting “self-healing” properties of the pulse to local perturbations of the medium, since the waves are coming from oblique directions and the center of the “X” can adjust to small medium perturbations and reform.

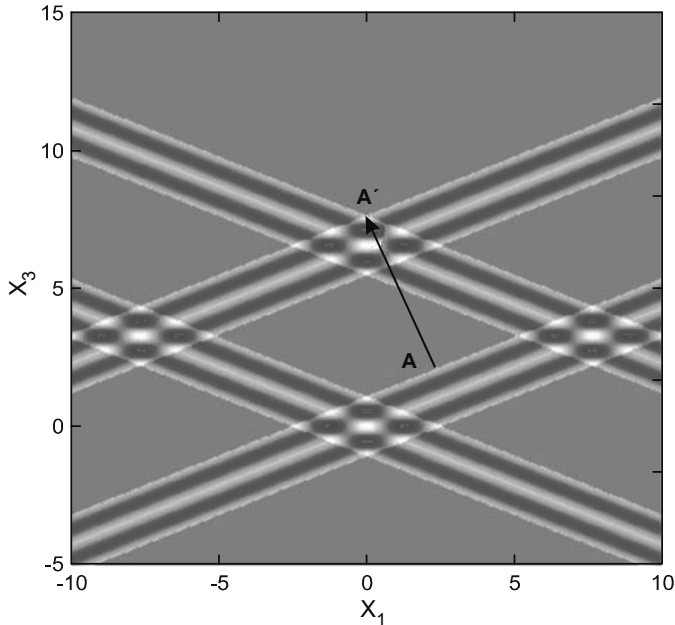


Fig. 6. A simplified X-shaped pulse formed by the crossing of two oblique plane waves at two different times moving in the vertical direction. The center of the “X” at different times comes from different parts of the two plane waves (adapted from Sauter and Paschke, 2001). The propagation axis is x_3 , where x_1 is the transverse coordinate and both are in arbitrary distance units.

In addition to Bessel beams in free space, a number of “paradoxes” have been found in “exotic media” where faster than light propagation have been inferred in recent years. For example, Wang *et al.* (2000) found superluminal light propagation in gain-assisted media. In examples like these, more elaborate explanations are required for large apparent velocities along the beam axis. Also, there have been inferences of ultra-slow light propagation in special media, for example by Vertergaard *et al.* (1999). A number of examples of fast and slow light have been summarized by Milonni (2005). How these results will ultimately be interpreted and if they have potential applications in seismology and geophysics is yet to be determined. However, as discussed by Zamboni-Rached *et al.* (2010), the central intensity peaks of a simple X-wave at different locations are not causally related instead being fed by waves coming from different parts of the incident aperture plane traveling with at most luminal speeds. As a result, Zamboni-Rached *et al.* (2010) note that the primary interest in superluminal X-waves has been with regard to their localization as well as self-reconstruction properties, and not in transmitting actual information superluminally.

In addition to superluminal localized wave solutions, localized waves have been described with central peak velocities ranging from 0 to infinity (Recami and Zamboni-Rached, 2009, 2011). Subluminal localized waves of the wave equation were described by Zamboni-Rached and Recami (2008) which in the simplest cases have ball-like shapes, in contrast to the X-wave shapes of superluminal localized waves. In addition, Zamboni-Rached *et al.* (2004) described so-called frozen waves to model a wide range of longitudinal (on-axis) and transverse intensity profiles by a summation of Bessel beams with different longitudinal wavenumbers (see also, Zamboni-Rached *et al.*, 2008).

4. BESSEL-GAUSS BEAMS AS LIMITED DIFFRACTION LOCALIZED WAVES

Realizable Bessel beams must ultimately be truncated by an aperture which will result in a limited distance over which diffraction-free propagation will occur. For a Gaussian tapered Bessel beam profile, Gori *et al.* (1987) (see also earlier work by Sheppard and Wilson, 1978) derived an analytic solution for a Bessel-Gauss beam. The initial amplitude profile at $x_3 = 0$ is

$$u(r, 0) = AJ_0(\beta r)e^{-(r/W_0)^2}, \tag{19}$$

and a solution at a distance x_3 is then

$$u(r, x_3) = \frac{AW_0}{W(x_3)} e^{i\left[\left(k - \frac{\beta^2}{2k}\right)x_3 - \psi(x_3)\right]} J_0\left(\frac{\beta r}{1 + \frac{ix_3}{X_3^R}}\right) e^{\left(\frac{-1}{W^2(x_3)} + \frac{ik}{2R(x_3)}\right)\left(r^2 + \beta^2 \frac{x_3^2}{k^2}\right)}, \tag{20}$$

where X_3^R is the Rayleigh range, and $W(x_3)$, $\psi(x_3)$ and $R(x_3)$ are the beam-width, the phase-shift and the radius of curvature for an ordinary Gaussian beam, respectively

(Gori *et al.*, 1987). For the underlying Bessel beam, $\beta = k \sin \theta$, and when $\beta = 0$ it will reduce to a Gaussian beam. For $W_0 \rightarrow \infty$, it reduces to an ideal diffraction-free Bessel beam.

Palma (1997) described Bessel-Gauss beams as a superposition of ordinary Gaussian beams with central rays along a fixed cone angle from the propagation direction of the Bessel-Gauss beam. Bessel-Gauss beams can therefore either be described as a Gaussian tapered Bessel beam or as a summation of tilted Gaussian beams along a fixed cone of directions. For heterogeneous media, paraxial ray theory (or dynamic ray tracing as utilized in seismology) can be used to track Bessel-Gauss beams in a similar fashion as Gaussian beams (Turunen and Friberg, 2010).

The far-zone angular spread of an individual Gaussian beam is $\theta_G = \lambda/\pi W_0$, and the ratio of θ_G and the cone angle of the Bessel beam will be $\theta/\theta_G = (\pi W_0/\lambda) \sin^{-1}(\beta/k) \approx \beta W_0/2$. When $\theta/\theta_G < 1$ is small, then W_0 will be comparable or smaller than the central lobe of the Bessel beam with a radius of $W_{bb} = 2.4/\beta$, and as a result the outer rings of the Bessel function will be truncated and the wave will approximate a Gaussian beam. When $\theta/\theta_G > 1$ then W_0 will be larger and the cone of Gaussian beams will overlap out to a distance D_{bb} over which the field will behave more like a Bessel beam. Gori *et al.* (1987) gave this distance to be approximately $D_{bb} \sim W_0/\theta$.

As an example using appropriate seismological parameters, Fig. 7 shows the transverse amplitude profiles of a Bessel-Gauss beam at several propagation distances. The medium speed is specified to be 5 km/s and the frequency is 1 Hz. For this example, the radius of the central lobe of the Bessel-Gauss beams W_{bb} is 4.5 km comparable to the wavelength, and the Gaussian beam width W_0 is 30 km, or about 6.6 times larger than W_{bb} . For this case, the Bessel beam retains its shape out to a distance of about 69 km, or about 15 times the radius of the central lobe of the underlying Bessel beam.

5. DISCUSSION AND CONCLUSIONS

In this overview, the basic properties of Gaussian beams and Bessel beams have been described. Gaussian beams are examples of non-localized beam solutions that can be used to concentrate and focus wave energy at the beam-waist, but still diffract for other distance ranges. In contrast, Bessel beams are localized beam solutions that have a transverse pattern which is stationary with propagation distance and are therefore non-diffracting. For Bessel beams, however, the energy is distributed among the different concentric rings making up the beam, and is not all concentrated on the central lobe. Fig. 8 shows a qualitative comparison of a Gaussian beam with a Bessel beam truncated by an aperture (from Salo and Friberg, 2008). For this case, the central lobe of the diffraction-free beam has about the same width as the focused beam-waist of the Gaussian beam. However, the Gaussian beam diffracts for other distance ranges and the Bessel beam is ultimately limited by the aperture. Nonetheless, the central lobe of a Bessel beam can be made very compact, and Bessel beams have been used in optics for directional pointing toward small objects, such as individual atoms, or used as atomic tweezers.

Bessel beams also have the ability to reform from small medium perturbations along the central beam (Turunen and Friberg, 2010).

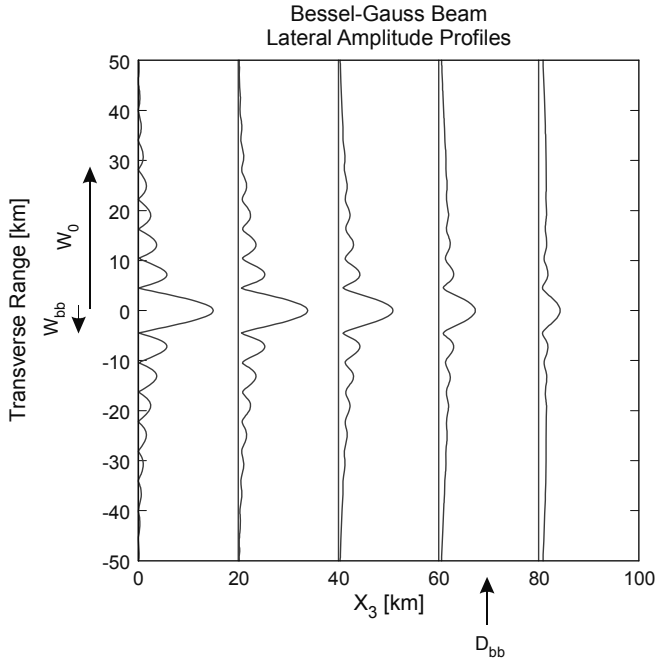


Fig. 7. An example of a Bessel-Gauss beam resulting from a Gaussian tapered Bessel beam. The medium speed is 5 km/s and the frequency is 1 Hz. For this case, the wavelength is 5 km, the radius of the central Bessel beam lobe W_{bb} is 4.5 km and the Gaussian beam width W_0 is 30 km. The Bessel beam retains its shape out to a distance D_{bb} of 69 km.

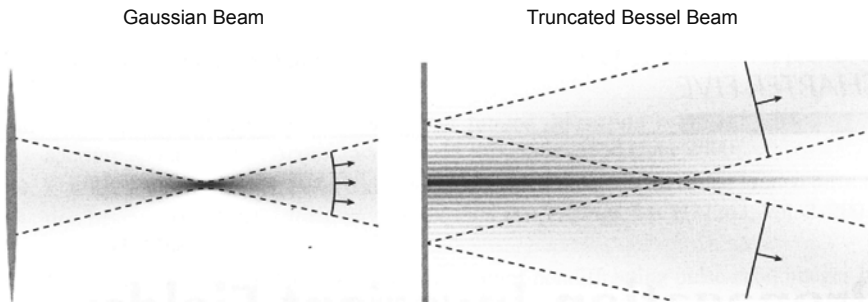


Fig. 8. A comparison between a Gaussian beam and a finite-aperture limited-diffraction Bessel beam. For this example, the maximum of the central lobe of the Bessel beam has about the same width as the beam waist of the Gaussian beam (adapted from Salo and Friberg, 2008).

In medical acoustics, *Lu and Greenleaf (1994)* contrasted ultrasonic beam forming using both focused Gaussian beams and limited diffraction beams (see also *Lu, 2008*). However, a disadvantage in the use of limited diffraction beams is the large side-lobes compared to Gaussian beams, but there have been efforts in medical acoustics to address this (*Lu and Greenleaf, 1995*). *Lu and Liu (2000)* described an X-wave transform in which wavefields can be decomposed into limited diffraction X-waves. *Lu (1997)* also described a pulse-echo imaging method utilizing limited diffraction beams in medical ultrasound. In seismology and geophysics, the decomposition of reflection wavefields into localized Gaussian beams have been used successfully for the migration imaging of seismic reflection data. Because of the similarities between acoustics and seismics, there could also be potentially important applications of limited diffraction beams in seismic imaging because of their advantages in terms of controllability and wide depth of focus. However, uses of limited diffraction beam solutions in seismology and geophysics are just beginning to be explored.

Acknowledgements: This work was supported in part by the National Science Foundation grant EAR06-35611 and the Air Force Geophysics Laboratory contract FA8718-08-C-002 and partly by the members of the Geo-Mathematical Imaging Group (GMIG) at Purdue University. I would also like to thank the three anonymous reviewers for their constructive comments.

References

- Aki K. and Richards P., 1980. *Quantitative Seismology*. W.H. Freeman, San Francisco, CA.
- Alkhalifah T., 1995. Gaussian beam depth migration for anisotropic media. *Geophysics*, **60**, 1474–1484.
- Babich V.M. and Popov M.M., 1989. Gaussian beam summation (review). *Izvestiya Vysshikh Uchebnykh Zavedenii Radiofizika*, **32**, 1447–1466 (in Russian, translated in *Radiophysics and Quantum Electronics*, **32**, 1063–1081, 1990).
- Bateman H., 1915. *Electrical and Optical Wave Motion*. Cambridge University Press, Cambridge, U.K.
- Bouchal Z., 2003. Nondiffracting optical beams: physical properties, experiments, and applications. *Czech J. Phys.*, **53**, 537–578.
- Brillouin L., 1960. *Wave Propagation and Group Velocity*. Academic Press, New York.
- Brittingham J.N., 1983. Focus wave modes in homogeneous Maxwell's equations: transverse electric mode. *J. Appl. Phys.*, **54**, 1179–1189.
- Burckhardt C.B., Hoffmann H. and Grandchamp P.-A., 1973. Ultrasound axicon: a device for focusing over a large depth. *J. Acoust. Soc. Am.*, **54**, 1628–1630.
- Červený V., 2001. *Seismic Ray Theory*. Cambridge University Press, Cambridge, U.K.
- Červený V., Klimeš and Pšenčík I., 2007. Seismic ray method: recent developments. *Adv. Geophys.*, **48**, 1–128.
- Červený V., Popov M.M. and Pšenčík I., 1982. Computation of wavefields in inhomogeneous media - Gaussian beam approach. *Geophys. J. R. Astr. Soc.*, **70**, 109–128.
- Chavez-Cerda S., 1999. A new approach to Bessel beams. *J. Mod. Opt.*, **46**, 923–930.
- Chew W.C., 1990. *Waves and Fields in Inhomogeneous Media*. Van Nostrand Reinhold, New York.
- Courant R. and Hilbert D., 1966. *Methods of Mathematical Physics, Vol. 2*. Wiley, New York.

- Deschamps G.A., 1971. Gaussian beams as a bundle of complex rays. *Electron. Lett.*, **7**, 684–685.
- de Hoop M.V., Smith H., Uhlmann G. and van der Hilst R.D., 2009. Seismic imaging with the generalized Radon transform: a curvelet transform perspective. *Inverse Probl.*, **25**, 025005, DOI: 10.1088/0266-5611/25/2/025005.
- Douma H. and de Hoop M.V., 2007. Leading-order seismic imaging using curvelets. *Geophysics*, **72**, S231–S248.
- Durnin J., 1987. Exact solutions for nondiffracting beams: I. the scalar theory. *J. Opt. Soc. Am. A*, **4**, 651–654.
- Durnin J., Miceli J.J. and Eberly J.H., 1987. Diffraction-free beams. *Phys. Rev. Lett.*, **58**, 1499–1501.
- Felsen L.B., 1976. Complex-source-point solutions of the field equations and their relation to the propagation and scattering of Gaussian beams. *Symp. Matemat.*, **18**. Istituto Nazionale di Alta Matematica, Academic Press, London, 40–56.
- Feng S. and Winful H.G., 2001. Physical origin of the Gouy shift. *Opt. Lett.*, **26**, 485–487.
- Flammer C., 1957. *Spheroidal Wave Functions*. Stanford Press, Stanford, CA.
- Gori F., Guattari G. and Padovani C., 1987. Bessel-Gauss beams. *Optics Commun.*, **64**, 491–495.
- Gray S.H., 2005. Gaussian beam migration of common-shot records. *Geophysics*, **70**, S71–S77.
- Gray S.H. and Bleistein N., 2009. True-amplitude Gaussian-beam migration. *Geophysics*, **74**, S11–S23.
- Hill N.R., 1990. Gaussian beam migration. *Geophysics*, **55**, 1416–1428.
- Hill N.R., 2001. Prestack Gaussian beam depth migration. *Geophysics*, **66**, 1240–1250.
- ISGILW-Sanya2011, 2011. *International Symposium on Geophysical Imaging with Localized waves*. <http://es.ucsc.edu/~acti/sanya/>.
- Keller J.B. and Streifer W. 1971. Complex rays with applications to Gaussian beams. *J. Opt. Soc. Am.*, **61**, 41–43.
- Kravtsov Yu.A. and Berczynski P., 2007. Gaussian beams in inhomogeneous media: a review. *Stud. Geophys. Geod.*, **51**, 1–36.
- Lu J.Y., 1997. 2D and 3D high frame rate imaging with limited diffraction beams. *IEEE Trans. Ultrason. Ferroelectr. Freq. Control*, **44**, 839–856.
- Lu J.Y., 2008. Ultrasonic imaging with limited-diffraction beams. In: Hernandez-Figueroa H.E., Zamboni-Rached M. and Recami E. (Eds.), *Localized Waves*. Wiley Interscience, New York, 97–128.
- Lu J.Y. and Greenleaf J.F., 1992a. Nondiffracting X-waves: exact solution to free-space scalar wave equation and their finite aperture realizations. *IEEE Trans. Ultrason. Ferroelectr. Freq. Control*, **39**, 19–31.
- Lu J.Y. and Greenleaf J.F., 1992b. Experimental verification of nondiffracting X-waves. *IEEE Trans. Ultrason. Ferroelectr. Freq. Control*, **39**, 441–446.
- Lu J.Y. and Greenleaf J.F., 1994. Biomedical ultrasound beam forming. *Ultrasound Med. Biol.*, **20**, 403–428.
- Lu J.Y. and Greenleaf J.F., 1995. Comparison of sidelobes of limited diffraction beams and localized waves. In: Jones J.P. (Ed.), *Acoustic Imaging, Vol. 21*. Plenum Press, New York, 145–152.
- Lu J.Y. and Liu A., 2000. An X wave transform. *IEEE Trans. Ultrason. Ferroelectr. Freq. Control*, **47**, 1472–1481.
- Lunardi J.T., 2001. Remarks on Bessel beams, signals and superluminality. *Phys. Lett. A*, **291**, 66–72.

- McDonald K.T., 2000. Bessel beams. www.hep.princeton.edu/mcdonald/examples/.
- McDonald K.T., 2002. Gaussian laser beams via oblate spheroidal waves. www.hep.princeton.edu/mcdonald/examples/.
- McGloin D. and Dholakia K., 2005. Bessel beams: diffraction in a new light. *Contemp. Phys.*, **46**, 15–28.
- McLeod J.H., 1954. The axicon: a new type of optical element. *J. Opt. Soc. Am.*, **44**, 592–597.
- McLeod J.H., 1960. Axicons and their uses. *J. Opt. Soc. Am.*, **50**, 166–169.
- Milonni P.W., 2005. *Fast Light, Slow Light and Left-Handed Light*. Institute of Physics Publ. Bristol, U.K.
- Mugnai D., Ranfagni A. and Ruggeri R., 2000. Observation of superluminal behaviors in wave propagation. *Phys. Rev. Lett.*, **84**, 4830–4833.
- Nowack R.L., 2003. Calculation of synthetic seismograms with Gaussian beams. *Pure Appl. Geophys.*, **160**, 487–507.
- Nowack R.L., 2008. Focused Gaussian beams for seismic imaging. *SEG Expanded Abstracts*, **27**, 2376–2380.
- Nowack R.L., 2011. Dynamically focused Gaussian beams for seismic imaging. *Int. J. Geophys.*, 316581, DOI: 10.1155/2011/316581.
- Nowack R.L. and Kainkaryam S.M., 2011. The Gouy phase anomaly for harmonic and time-domain paraxial Gaussian beams. *Geophys. J. Int.*, **184**, 965–973.
- Nowack R.L., Sen M.K. and Stoffa P.L., 2003. Gaussian beam migration of sparse common-shot data. *SEG Expanded Abstracts*, **22**, 1114–1117.
- Palma C., 2001. Decentered Gaussian beams, ray bundles and Bessel-Gauss beams. *Appl. Optics*, **36**, 1116–1120.
- Popov M.M., 1982. A new method of computation of wave fields using Gaussian beams. *Wave Motion*, **4**, 85–97.
- Popov M.M., 2002. *Ray Theory and Gaussian Beam Method for Geophysicists*. Lecture Notes, University of Bahia, Salvador, Brazil.
- Popov M.M., Semtchenok N.M., Popov P.M. and Verdel A.R., 2010. Depth migration by the Gaussian beam summation method. *Geophysics*, **75**, S81–S93.
- Protasov M.I. and Cheverda V.A., 2006. True-amplitude seismic imaging. *Dokl. Earth Sci.*, **407**, 441–445.
- Protasov M.I. and Tcheverda V.A., 2011. True amplitude imaging by inverse generalized Radon transform based on Gaussian beam decomposition of the acoustic Green's function, *Geophys. J. Int.*, **59**, 197–209.
- Recami E., 1998. On localized “X-shaped” superluminal solutions to Maxwell equations. *Physica A*, **252**, 586–610.
- Recami E. and Zamboni-Rached M., 2009. Localized waves: a review. *Adv. Imag. Electron Phys.*, **156**, 235–353.
- Recami E. and Zamboni-Rached M., 2011. Non-diffracting waves, and “frozen waves”: an introduction. *International Symposium on Geophysical Imaging with Localized Waves*, Sanya, China, July 24–28 2011, <http://es.ucsc.edu/~acti/sanya/SanyaRecamiTalk.pdf>.
- Recami E., Zamboni-Rached M. and Hernandez-Figueroa H.E., 2008. Localized waves: a historical and scientific introduction. In: Hernandez-Figueroa H.E., Zamboni-Rached M. and Recami E. (Eds.), *Localized Waves*. Wiley Interscience, New York, 1–41.
- Saari P. and Reivelt K., 1997. Evidence of X-shaped propagation-invariant localized light waves. *Phys. Rev. Lett.*, **79**, 4135–4138.

- Salo J. and Friberg A.T., 2008. Propagation-invariant fields: rotationally periodic and anisotropic nondiffracting waves. In: Hernandez-Figueroa H.E., Zamboni-Rached M. and Recami E. (Eds.), *Localized Waves*. Wiley Interscience, New York, 129–157.
- Sauter T. and Paschke F., 2001. Can Bessel beams carry superluminal signals? *Phys. Lett. A*, **285**, 1–6.
- Sheppard C.J.R., 1978. Electromagnetic field in the focal region of wide-angular annular lens and mirror systems. **2**, 163–166.
- Sheppard C.J.R. and Wilson T., 1978. Gaussian-beam theory of lenses with annular aperture. *Microwaves, Optics and Acoustics*, **2**(4), 105–112.
- Siegman A.E., 1986. *Lasers*. University Science Books, Sausalito, CA.
- Stratton J.A., 1941. *Electromagnetic Theory*. McGraw-Hill, New York.
- Stratton J.A., 1956. *Spheroidal Wave Functions*. Wiley, New York.
- Turunen J. and Friberg A., 2010. Propagation-invariant optical fields. *Progress in Optics*, **54**, 1–88.
- Vertergaard Hau L., Harris S.E., Dutton Z. and Behroozi C.H., 1999. Light speed reduction to 17 metres per second in an ultracold atomic gas. *Nature*, **397**, 594–598.
- Walker S.C. and Kuperman W.A., 2007. Cherenkov-Vavilov formulation of X waves. *Phys. Rev. Lett.*, **99**, 244802.
- Wang L.J., Kuzmich A. and Dogariu A., 2000. Gain-assisted superluminal light propagation. *Nature*, **406**, 277–279.
- Weber H.J. and Arfken G.B., 2004. *Essential Mathematical Methods for Physicists*. Elsevier, Amsterdam, The Netherlands.
- Wu R.S., 1985. Gaussian beams, complex rays, and the analytic extension of the Green's function in smoothly inhomogeneous media. *Geophys. J. R. Astr. Soc.*, **83**, 93–110.
- Wu T.T., 1985. Electromagnetic missiles. *J. Appl. Phys.*, **57**, 2370–2373.
- Žáček, K., 2006. Decomposition of the wavefield into optimized Gaussian packets. *Stud. Geophys. Geod.*, **50**, 367–380.
- Zamboni-Rached M. and Recami E., 2008. Subluminal wave bullets: Exact localized subluminal solutions to the wave equation. *Phys. Rev. A*, **77**, 033824.
- Zamboni-Rached M., Recami E. and Besieris I.M., 2010. Cherenkov radiation versus X-shaped localized waves. *J. Opt. Soc. Am. A*, **27**, 928–934.
- Zamboni-Rached M., Recami E. and Hernandez-Figueroa H.E., 2002. New Localized superluminal solutions to the wave equations with finite total energies and arbitrary frequencies. *Eur. Phys. J. D*, **21**, 217–228.
- Zamboni-Rached M., Recami E. and Hernandez-Figueroa H.E., 2004. Theory of frozen waves: modelling the shape of stationary wave fields. *J. Opt. Soc. Am. A*, **22**, 2465–2475.
- Zamboni-Rached M., Recami E. and Hernandez-Figueroa H.E., 2008. Structure of nondiffracting waves and some interesting applications. In: Hernandez-Figueroa H.E., Zamboni-Rached M. and Recami E. (Eds.), *Localized Waves*. Wiley Interscience, New York, 43–77.
- Zheng Y., Geng Y. and Wu R.S., 2011. Numerical investigation of propagation of localized waves in complex media. *International Symposium on Geophysical Imaging with Localized Waves*, Sanya, China, July 24–28, 2011, <http://es.ucsc.edu/~yzheng/sanya/>.
- Ziolkowski R.W., 1985. Exact solutions of the wave equation with complex source locations. *J. Math. Phys.*, **26**, 861–863.